

Chapter 2

High-Temperature Superconductivity

2.1 Introduction

The discovery of high-temperature superconductivity at 30K in the La-Ba-Cu-O system in 1986 by Bednorz and Müller (Bednorz and Müller,1986) took the world by surprise that a copper oxide alloy is able to conduct electricity with zero resistance at high temperature. They found that LaBaCuO is superconducting up to 35 K. Chu's group (Wu et al.,1987) found that applied pressure elevates T_c in the La-based cuprate and discovered the superconductor YBaCuO with a transition temperature near 90K which is above the boiling point of liquid nitrogen(77K).

During the past decade of research on this subject, significant progress has been made on both the fundamental science and technological application fronts. For example, the symmetry of the superconducting order parameter is established and the superconducting pairing mechanism is on the threshold of being identified. Prospects seem to be good for attaining a fundamental understanding of high-temperature superconductors and realizing technological applications of these materials on a broad scale during the next decade.

2.2 High- T_c Superconducting Cuprates

The dramatic increases in T_c that have been observed since 1986 are illustrated in Fig. 2.1 where the maximum value of T_c is plotted versus date. Prior to 1986, the A15 compound Nb_3Ge with $T_c = 23K$ held the record for the highest value of T_c . After the important discoveries of Chu's group, interest became

focused on two series of compounds both showed superconductivity above 100K. Maeda's group (Maeda et al., 1988) first reported the existence of a superconducting phase with T_c of around 105K in BaSrCaCuO. The structure and properties of this system was intensively studied by Chu's group (Hazen et al., 1988). It was established that the new series of superconductors has the structural formula type $Bi_2Sr_2Ca_{n-1}Cu_nO_{2n+4}$ with T_c of 10, 85, and 110K for $n = 1, 2, 3$ respectively. Shortly afterwards Sheng and Hermann (Sheng and Hermann, 1988) announced superconductivity above 100K in the system TlBaCaCuO. The structural formula of this system is $Tl_2Ba_2Ca_{n-1}Cu_nO_{2n+4}$ with T_c of 80, 110, and 125K for $n = 1, 2,$ and 3 respectively. The maximum value of T_c has increased to its present value of 133K for a compound in the HgBaCaCuO system. When this compound $HgBa_2Ca_2Cu_3O_8$ is subjected to high pressure, the onset of T_c increases to 164K at pressure 30 GPa. Value of T_c in excess of the boiling point of liquid nitrogen immediately indicates high- T_c cuprates as promising candidates for technological applications of superconductivity since the cuprate materials have the advantage that they can be cooled into the superconducting state using liquid nitrogen.

Approximately 100 different cuprate materials, many of which are superconducting, have been discovered since 1986. Several of the more important high- T_c cuprate superconductors are listed in Table 2.1 along with the maximum values of T_c observed in each class of materials. The abbreviated name for specific cuprate materials are included.

2.3 Structure and Charge-Carrier Doping

The high- T_c cuprate superconductors have layered perovskite-like crystal structures which consist of conducting CuO_2 planes separated by layers comprised of other elements A and oxygen, A_mO_n , and, in some cases, layers of Ln ions. The mobile charges carriers, which can be electrons but are usually holes, are believed to reside primarily within the CuO_2 planes. The A_mO_n layers apparently

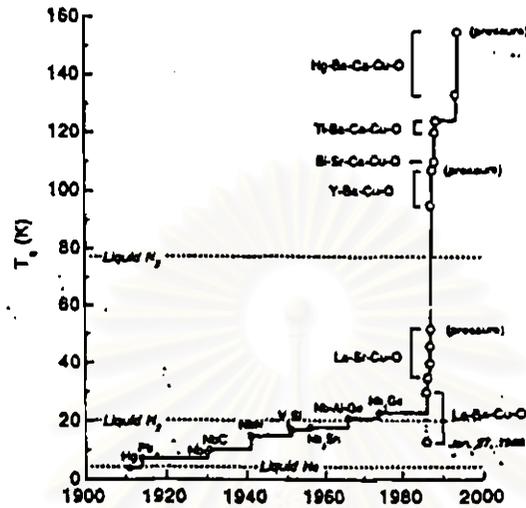


Figure 2.1: Maximum superconducting critical temperature versus date. (From Maple, 1998)

Table 2.1: High- T_c cuprate superconductors with the maximum values of T_c . (From Maple, 1998)

Material ($n=1,2,3,4$)	Abbreviated name	Max. $T_c(K)$
$La_{2-x}Sr_xCuO_4$	LSCO	40
$YBa_2Cu_3O_{7-\delta}$	YBCO	92
$Bi_2Sr_2Ca_{n-1}Cu_nO_{2n+4}$	BSCCO	110
$Tl_2Ba_2Ca_{n-1}Cu_nO_{2n+4}$	($n=3$)TBCCO	($n=3$) 122
$HgBa_2Ca_{n-1}Cu_nO_{2n+4}$	($n=3$)HBCCO	($n=3$)133

function as charge reservoirs and control the doping of the CuO_2 planes with charge carriers. In several of the compounds containing Ln layers, the Ln ions have been found to order antiferromagnetically at low temperatures. Many of the cuprates can be doped with charge carriers and made superconducting by substitution of appropriate elements into an antiferromagnetic insulating parent compound. The temperature T versus x phase diagrams for the $\text{La}_{2-x}\text{Sr}_x\text{CuO}_4$ and $\text{Nd}_{2-x}\text{Ce}_x\text{CuO}_{4-y}$ systems are shown in Fig. 2.2, and the corresponding crystal structures of the La_2CuO_4 and Nd_2CuO_4 parent compounds are displayed in Fig. 2.3. The $\text{La}_{2-x}\text{Sr}_x\text{CuO}_4$ and $\text{Nd}_{2-x}\text{Ce}_x\text{CuO}_{4-y}$ systems have one CuO_2 plane per unit cell. Other superconducting cuprate systems have more than one CuO_2 planes per unit cell: $\text{LnBa}_2\text{Cu}_3\text{O}_{7-x}$ has two CuO_2 planes per unit cell, while $\text{Bi}_2\text{Sr}_2\text{Ca}_{n-1}\text{Cu}_n\text{O}_x$ has n CuO_2 layers per unit cell and can be synthesized by conventional methods for $n=1,2,3$.

Two features in Fig.2.2 appear to be relevant to cuprate superconductivity: (1) the apparent electron-hole symmetry seems to provide a constraint on viable theory of high- T_c superconductivity in cuprates, and (2) the proximity of antiferromagnetism suggests that superconducting electron pairing in the cuprates is mediated by antiferromagnetic spin fluctuations. The occurrence of d-wave pairing is also consistent with the antiferromagnetic pairing mechanism.

2.4 Normal-State Properties

It is widely accepted that understanding the normal-state properties of the high- T_c cuprates will enlighten the superconducting mechanism. The normal state properties of the high- T_c cuprate superconductors are unusual and appear to violate the Landau Fermi-liquid theory. From the Fermi-liquid description of the normal state, we know that the magnetic susceptibility and the Hall coefficient are temperature independent, and the resistivity behaves like T^2 at low temperature. These behaviors have not been observed in the cuprates.

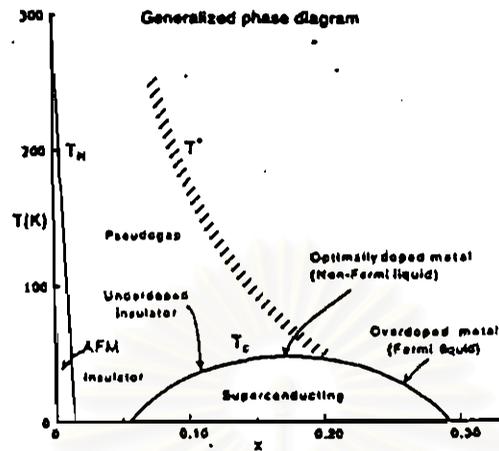


Figure 2.2: Temperature-dopant concentration (T - x) phase diagram. AFM=antiferromagnetic phase, SG=spin-glass phase, and SC=superconducting phase. (From Maple,1998.)

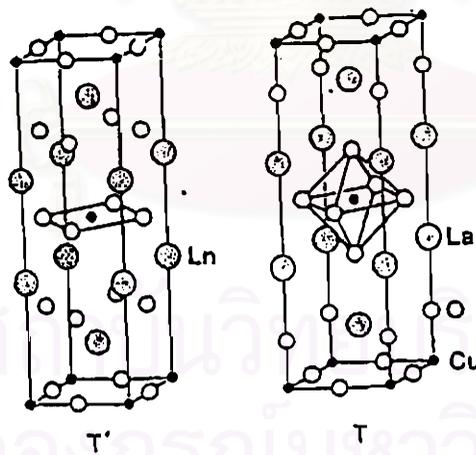


Figure 2.3: Crystal structure of La_2CuO_4 (T-phase) and Ln_2CuO_4 ($Ln=Pr,Nd,Sm,Eu,Gd$) T' phase, parent compound. (From Maple,1998)

In conventional low-temperature superconductors, the experimentally observed linear dependence of the resistivity ρ with temperature T obeys the formula $\rho = a + bT^5$ at low T but larger than T_c . This temperature dependence arises from the scattering of electrons with phonons. However, the behavior of in-plane electrical resistivity ρ observed in the high- T_c superconductors have an anomalous linear temperature dependence $\rho \approx T$ between T_c and high temperature 1000K. The Hall coefficient R_H is inversely proportional to T and the cotangent of the Hall angle $\theta_H = R_H/\rho$ varies as T^2 ; i.e. $\cot(\theta_H) = AT^2 + B$ (Chien, Wang, Ong, 1991). The linear T -dependence of $\rho(T)$ and the the quadratic T -dependence of $\cot\theta_H$ have been attributed to longitudinal and transverse scattering rates τ_l^{-1} and τ_t^{-1} that vary as T and T^2 , respectively.

The most remarkable aspect of the normal state is the pseudogap in the charge and spin-excitation spectra of under-doped cuprates. The pseudogap has been inferred from features in various transport, magnetic, and thermal measurements including $\rho(T)$, $R_H(T)$ (Hwang et al., 1994), thermoelectric power $S(T)$ (Tallon et al, 1995), NMR knight shift $K(T)$ (Warren et al., 1989), NMR spin lattice relaxation rate $1/T_1(T)$ (Takigawa et al., 1991), magnetic susceptibility (Hwang et al., 1994), neutron scattering (Rossat-Mignod et al., 1991), specific heat $C(T)$ (Loram et al., 1993), and angle-resolved photoemission spectroscopy ARPES (Ding et al., 1996).

The ARPES measurements reveal several striking aspects of the pseudogap. The magnitude of the pseudogap has the same k -dependence in the in-plane as the magnitude of the superconducting energy gap. The symmetry of the energy gap is consistent with $d_{x^2-y^2}$ symmetry inferred from Josephson tunneling measurements. The pseudogap and the superconducting energy gap appear to be intimately related to one another, with the former the precursor of the latter. These results support the view that a unified theory of both the normal and

superconducting states of the cuprates is needed.

2.5 Symmetry of Superconducting Order Parameter

During the last several years, a great deal of effort has been expended to determine the symmetry of the superconducting order parameter of the high- T_c superconductors (Levi, 1996). The pairing symmetry provides clues to the identity of the superconducting pairing mechanism which is essential for the development of the theory of high temperature superconductivity in the cuprates. The discovery of high- T_c superconductivity established from flux quantization, Josephson effect, and NMR measurements, that the superconductivity involves electrons that are paired in singlet spin state. Possible orbital pairing states include s-wave state, extended s-wave state and d-wave state. In the s-wave state, the energy gap $\Delta(\vec{k})$ is isotropic; i.e., $\Delta(\vec{k})$ is constant over the Fermi surface. For the extended s-wave state, the energy gap $\Delta(\vec{k})$ is anisotropic; i.e., $\Delta(\vec{k})$ exhibits a variation over the Fermi surface which has the same symmetry as the rotational symmetry of the crystal. Similarly, the energy gap $\Delta(\vec{k})$ for the d-wave case is anisotropic and can be expressed as $\Delta(\vec{k}) = \Delta_0[\cos(k_x a) - \cos(k_y a)]$. For both the extended s-wave and d-wave cases, $\Delta(\vec{k})$ vanishes at lines on the Fermi surface, resulting in a density of states $N_s(E)$ that is linear in energy E for low values of E . This leads to power law T^n (n =integer) behavior of the physical properties for $T \ll \Delta$; e.g., $C_c(T) \sim T^2$, the penetration depth $\lambda(T) \sim T$, and $1/T_1(T) \sim T^3$. The establishment of the order parameter requires the determination of both the magnitude and the phase of $\Delta(\vec{k})$. Shown in Fig.2.4 is a schematic diagram of the variation of the energy gap over Fermi surface and the density of states $N(E)$ versus E for the s-, extended s-, and d-states.

A number of different types of measurements have been performed on the high- T_c cuprate superconductors which are sensitive to the phase of $\Delta(\vec{k})$. These

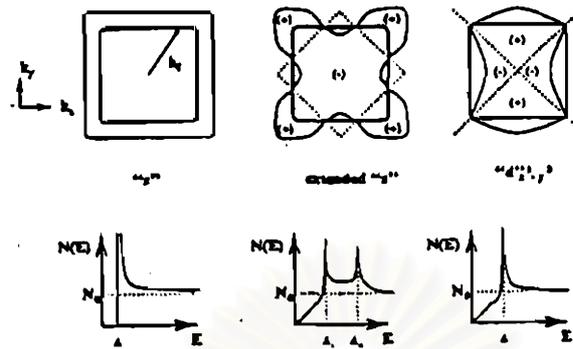


Figure 2.4: Fermi surface gap functions and densities of states of a superconductor with tetragonal symmetry for various pairing symmetries. Left: The s-wave with the constant gap. Middle: The extended s-wave. Right: A d-wave function of $d_{x^2-y^2}$ symmetry. (From Maple, 1998)

measurements involve the Josephson effect, include SQUID interferometry (Wollman et al., 1993), single junction modulation (Wollman et al., 1995), tricrystal ring magnetometry (Tsuei et al., 1994), c-axis Josephson tunneling (Sun et al., 1994), and grain boundary tunneling (Chaudhari and Lin, 1994). The SQUID interferometry, single-junction modulation, tricrystal ring magnetometry measurements were performed on YBCO. These experiments indicate that the superconducting order parameter has $d_{x^2-y^2}$ symmetry. However the c-axis Josephson tunneling studies on junctions consisting of a conventional superconductor (Pb) and twinned or untwinned single crystals of YBCO indicate that the superconducting order parameter has a significant s-wave component. The result provides strong evidence for mixed d- and s-wave pairing in YBCO and are consistent with predominant $d_{x^2-y^2}$ pairing symmetry.

2.6 Theories of Cuprate Superconductivity

To describe the behavior of the high- T_c materials, in this section we will write a Hamiltonian for these compounds. We begin with the electrons moving in

the CuO_2 plane. the copper ions Cu^{2+} have nine electrons in the five d orbitals, while O^{2-} has three p orbitals occupied. The state with the highest energy has mainly $d_{x^2-y^2}$ orbital and is unpaired that gives the ion a net spin 1/2. Thus in the absence of doping, each unit cell has a hole with a localized spin 1/2 state that causes antiferromagnetism. The other orbitals at lower energies are occupied, and will be neglected in the construction of the Hamiltonian.

When doping occurs, an additional electron is removed from the CuO_2 plane by the substitution of a La atom by a Sr atom in $La_{2-x}Sr_xCuO_4$. The x holes per cell is created and will be on oxygen sites, creating O^- . Since the copper atoms appear to keep the same valence state. It is possible to construct a Hamiltonian for an electron in the copper oxide planes. Using the hole notation where the vacuum is defined as filled $Cu(3d)^{10}$ and $O(2p)^6$ states. The Hamiltonian for a single layer of Cu and O atoms is given by (Zhang and Rice, 1988; Emery and Reiter, 1988)

$$H = \sum_{ij\sigma} \epsilon_{ij} a_{i\sigma}^\dagger a_{j\sigma} + \frac{1}{2} \sum_{ij\sigma\sigma'} U_{ij} a_{i\sigma}^\dagger a_{i\sigma} a_{j\sigma'}^\dagger a_{j\sigma'} \quad (2.1)$$

The fermionic operator $a_{i\sigma}^\dagger$ creates a hole with spin σ in the $2p_x$ and $2p_y$ orbital at the copper site i. The hole is in the $3d_{x^2-y^2}$ orbital of copper. The diagonal energy will be either (ϵ_p, U_p) or (ϵ_d, U_d) for the 2p or 3d state, respectively. The hopping energy term corresponds to the hybridization between the nearest neighbors Cu and O atoms.

Undoped La_2CuO_4 has 1 hole per copper atom, all the Cu sites are singly occupied and all the O sites are empty in the hole representation. The Hamiltonian (2.1) reduces to a spin 1/2 Heisenberg model on the square lattice of Cu sites:

$$H = J \sum_{\langle ij \rangle} \vec{S}_i \cdot \vec{S}_j \quad (2.2)$$

where (i,j) denotes the nearest-neighbor copper sites, \vec{S}_i are spin 1/2 operators, and J is a superexchange antiferromagnetic interaction between the neighboring copper sites.

Upon doping, additional holes introduced in the CuO_2 layers will go onto the oxygen sites since $U_d > \epsilon_p$. The added holes will cause the hybridization of Cu and O holes. Then the effective Hamiltonian for a single added hole is

$$H_{eff} = t \sum_{ij} a_{i\sigma}^\dagger a_{j\sigma} + J \sum_{ij} \vec{S}_i \cdot \vec{S}_j \quad (2.3)$$

This Hamiltonian is the so called t-J model (Zhang and Rice,1988; Emery and Reiter ,1988) in which the t and J are effectively independent parameters and it is a generalization of the exchange Hamiltonian for the non- half- filled- band case .

Previously, Anderson (Anderson,1987) has suggested that the CuO-based high- T_c superconducting oxides are materials with strong electron correlations and can be understood within a two-dimensional, large- U , single-band Hubbard model. Anderson's quantitative idea was led to the mean-field theory of Baskaran, Zou and Anderson (Baskaran, Zou and Anderson,1987). The ground state can be described by a correlated wave function of the form

$$|G\rangle = P \prod_{\vec{k}} (u_{\vec{k}} + v_{\vec{k}} a_{\vec{k}\uparrow}^\dagger a_{-\vec{k}\downarrow}^\dagger) |0\rangle \quad (2.4)$$

In this formula, P is the Gutzwiller projection onto the subspace of no-doubly-occupied sites. $u_{\vec{k}}$ and $v_{\vec{k}}$ are the usual BCS coherence factors for a momentum dependence gap function and are given by

$$u_{\vec{k}}^2 = \frac{1}{2} \left(1 + \frac{\xi_{\vec{k}}}{E_{\vec{k}}}\right), \quad v_{\vec{k}}^2 = \frac{1}{2} \left(1 - \frac{\xi_{\vec{k}}}{E_{\vec{k}}}\right) \quad (2.5)$$

where $E_{\vec{k}} = \sqrt{\xi_{\vec{k}}^2 + |\Delta|^2}$ is the quasi-particle energy in the superconducting state, $\xi_{\vec{k}} = -2t(\cos k_x + \cos k_y) - \mu$, μ is the chemical potential and $\Delta_{\vec{k}}$ is the superconducting gap function which gives the minimized ground state energy by choosing

the appropriate form of $\Delta_{\vec{k}}$. The average numbers of electrons are determined from the relation

$$N(1 - \delta) = \sum_{\vec{k}\sigma} \langle a_{\vec{k}\sigma}^\dagger a_{\vec{k}\sigma} \rangle \quad (2.6)$$

where N is the number of sites and $1 - \delta$ is the number of electron per sites.

After the canonical transformation , Baskaran, Zou and Anderson obtained the mean- field equation:

$$\Delta_{\vec{k}} = \sum_{\vec{k}'} V_{\vec{k}\vec{k}'} \frac{\Delta_{\vec{k}'}}{2E_{\vec{k}'}} \tanh(E_{\vec{k}'}/2T) \quad (2.7)$$

$$N(1 - \delta) = \sum_{\vec{k}} [1 - \frac{\xi_{\vec{k}}}{2E_{\vec{k}}} \tanh(E_{\vec{k}}/2T)] \quad (2.8)$$

$$V_{\vec{k}\vec{k}'} = J[\cos(k_x - k_{x'}) + \cos(k_y - k_{y'})] \quad (2.9)$$

here, T is the temperature . They also assumed the s-wave-like order parameter

$$\Delta_{\vec{k}} = \Delta_s(\cos k_x + \cos k_y) \quad (2.10)$$

with the crudest approximation for the hopping energy,t,i.e, $t = t_0\delta$, where t_0 is the bare hopping energy.

At half filling, $\delta = 0$ describes a disordered phase of the quantum Heisenberg antiferromagnet, e.g., the resonating valence bond (RVB) state. At finite δ , $|G\rangle$ describes a superconducting states that evolves from the insulating state at $\delta = 0$.

Unfortunately, the Gutzwiller projection can only be performed numerically (Gross, Joynt, and Rice , 1987). However, Ruckenstein, Hirshfeld and Appel (Ruckenstein, Hirshfeld and Appel, 1987) treating this problem by using the auxiliary- boson approach in the mean-field theory provided the equivalent between the Gutzwiller projection and the auxiliary- boson approach. Gotliar

(Gotliar,1988) extended the works of Baskaran, Zou and Anderson and Ruckenstein, Hirshfeld and Appel by considering the order parameter of the form

$$\Delta_{\vec{k}} = \Delta_s(\cos k_x + \cos k_y) + \Delta_d(\cos k_x - \cos k_y) \quad (2.11)$$

which represents a mixture of the s-wave-like and d-wave-like order parameters. They found that the stable solutions of the mean-field theory at half filling is a mixture state of the s-wave and d-wave order parameters, the transition temperature in each pairing channels have the same critical temperature at half filling and the zero temperature order parameter has the (s+id) state. Away from half filling the d-wave transition temperature has a higher critical temperature, the superconducting order parameter at low temperature is a mixture of the s-wave and the d-wave. However, these results are quantitatively important at very low hole concentrations and require a more sophisticated theoretical treatment.

Several theories have been proposed to describe the behavior of the high- T_c compound. One- and three- band Hubbard models (Hubbard, 1963), as well as the t-J model (Zhang and Rice, 1988), are believed to represent the feature of the electronic behavior of the new materials. Unfortunately, most of the experimental data are not accurate enough to confirm the theories. the antiferromagnetic property of the normal state may be combined with the pairing ideas to describe the high- T_c superconductors. In the spin bag theories Schrieffer, Wen, Zhang,1989; (Kampf and Schrieffer, 1990) considered a hole moving in a background that has a spin density wave (SDW). A local distortion of the SDW order would create a spin bag and these bags attracting to form Cooper pairs. In antiferromagnetic Fermi-liquid theories Millis, Monien, and Pines, 1990 performed a study of the NMR spectra to extract a phenomenological model for the spin susceptibility. This model invokes a strong enhancement of the spin susceptibility near a nesting momentum at very low frequency. The interchange of magnons may produce

the attractive force needed for the charge carriers (Miyake, Schmitt-Rink, and Varma, 1986). Among the Fermi-liquid-based theories one may include the Van Hove singularity scenario (Markiewicz, 1991; Newns, Pattnaik, and Tsuei, 1991), and the nested Fermi liquid (Virosztek and Ruvalds, 1990).



สถาบันวิทยบริการ
จุฬาลงกรณ์มหาวิทยาลัย